PHOENICS News

CHAM

This edition of the PHOENICS Newsletter contains contributions from PHOENICS Users showing how the software can be used to model, and improve, diverse environmental applications including the impact of cooking on air quality in China, improving energy conservation in homes with BIPV Façade Structures and assorted applications from Users in Germany. There is also a follow up to an article published 10 years ago regarding MOFOR. The next Newsletter will provide information on new features in, and improvements to, PHOENICS in its 2020 release.

Table of Contents

Winter 2019/2020

A related article by the author on modelling the 'Dead Water' effect was published in the PHOENICS Newsletter in 2009 (Ref 1). In that article, PHOENICS simulations were accomplished using a coordinate system fixed in the body so that an inflow velocity, corresponding to the predicted body speed, was applied in conjunction with a body force on the fluid. Figure 1a shows the 2m long experimental tank with lower fluid layer (white) of density 1025 kg/m-3 and upper layer (red) of density 1000kg/m-3. A rectangular block (0.12m long, 0.1m wide and 0.0275m deep) was towed through the fluid (from left to right) by means of a constant driving force. Figure 1a shows experimental results after 16s of towing the body from rest. The result of the corresponding PHOENICS simulation (blue showing lighter fluid and red heavier fluid) is shown in Figure 1b. It can be seen that there is reasonable agreement in the internal wave profiles between experiment and PHOENICS prediction.

PHOENICS has a moving body facility (MOFOR) which uses a surprisingly simple technique. The body is assumed filled with fluid which is constrained to move with body velocity. In PHOENICS this is accomplished by fixing the fluid in the body with the body velocity. The current MOFOR facility, however, assumes a specified position or velocity of the body as a function of time. It cannot therefore deal with a body that moves under application of a specified force (as would be required for this experiment). There is no reason, though, that the MOFOR concept cannot be adapted to model the experimental situation. This requires only that body velocities, computed from the equation of motion of the body, are fixed in GROUND. This modification has been carried out (tagged by my initials, RPH) and the results are now presented.
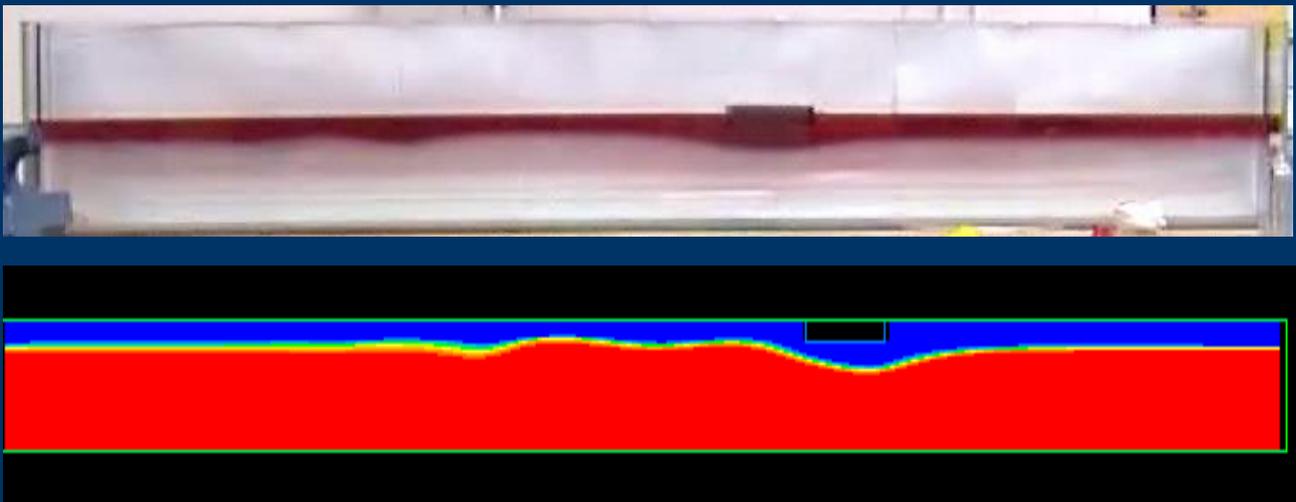

Figure 1. (a) Top, rectangular body is being towed left to right in a 2m long tank, 0.25m wide, filled with stratified fluid to a depth of 0.15m. The lower fluid layer (white) is salt water with density 1025 kg/m-3 and the upper layer fresh water with density 1000kg/m-3. Image courtesy of Professor Leo Maas of the Royal Netherlands Institute for Sea Research. (b) Bottom, PHOENICS simulation using a FIXED body. Here the lower density layer is coloured red and the upper layer coloured blue.

Methodology and Results

It has been considered wise to check both MOFOR and RPH for the simpler case of the above block moving in the tank filled with fluid of uniform density 1000kg/m-3. The prescribed motion chosen for the body is given by:

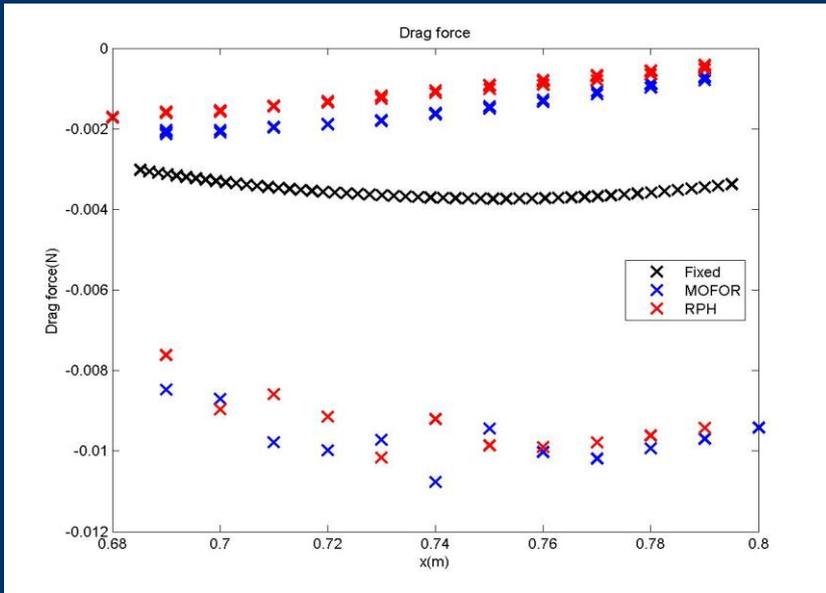$$x = at + \left(\frac{a}{\omega}\right)\sin(\omega t)$$

Figure 2. Comparison of the drag forces (Fixed (black), MOFOR (blue) and RPH (red)) on the body over a section of the tank
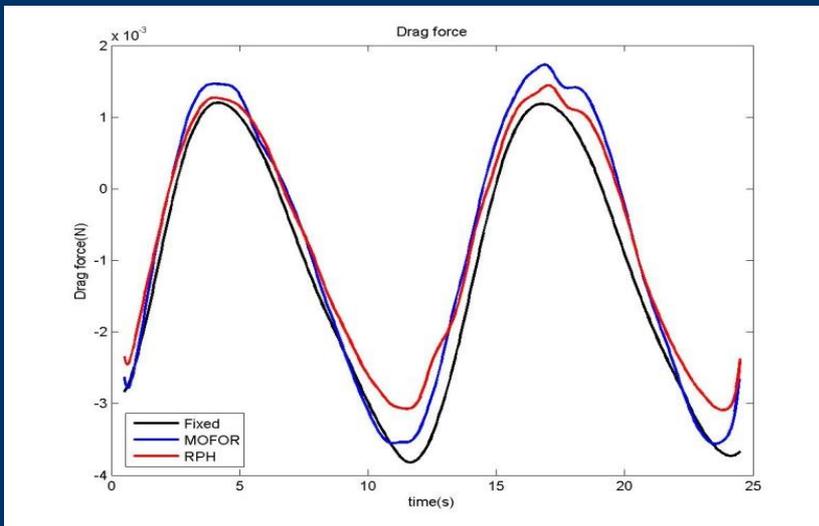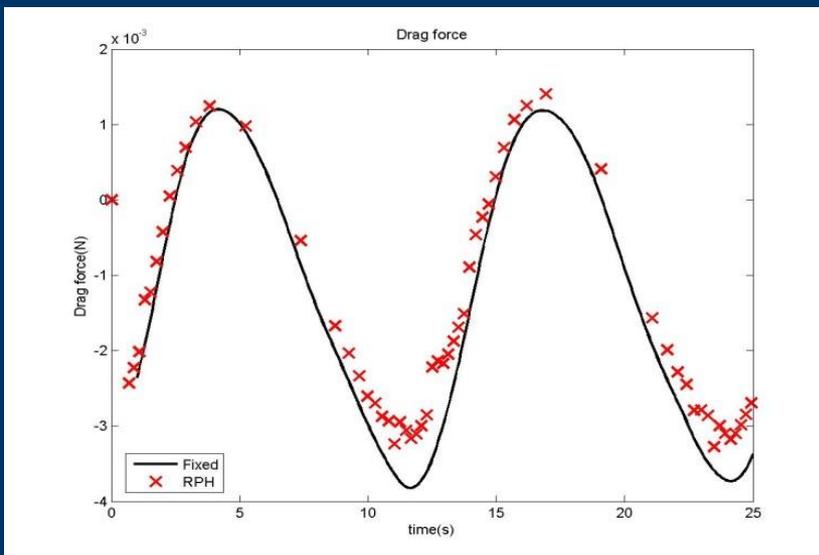

Figure 3 (a)

Figure 3 (b)

Where $a=0.025m/s$, $\omega=4\pi\iota/251\text{-}s$ and x (m) is the distance along the tank. The value of a is chosen to be represent velocities achieved in the experiment and ω is chosen using the transit time of the block as period. When looking at results for the forces on the body resulting from the motion for both MOFOR and RPH applications the forces oscillate which, initially, appears disturbing. Figure 2 shows the drag forces calculated by MOFOR and RPH compared with those using a fixed body over a 0.68m to 0.8m section of the tank.

On reflection, the oscillation in the forces may perhaps be expected as the body may spend several time steps within the same group of computational cells and a variation in the force may be necessary to be consistent with maintaining a fixed position. It should be noted that all other aspects of the simulations appear satisfactory (for example, the equation residuals are well behaved). However, a smoothing technique applied to the forces recovers reasonable agreement with the fixed body results as shown in Figure 3a. An in cell averaging technique for the forces has also been successfully tried, Figure 3b.

Figure 3a Top, Comparison of the smoothed RPH (red), MOFOR (blue) drag forces with the fixed body (black) results. Figure 3b Bottom, Comparison of the fixed body (black) results with the RPH (red) cell averaged results.

The RPH method has then been applied to the stratified tank experiment (see Figure 1a) where the body is towed with constant force from rest.

3

The equation of motion of the body is integrated to determine the body velocities and position at each time step. The predicted results in the stratified tank are shown in Figure 4 and should be compared with those in Figure 1. These preliminary-moving-body results have a much coarser grid than the fixed-body results but, even so, the results are encouraging.
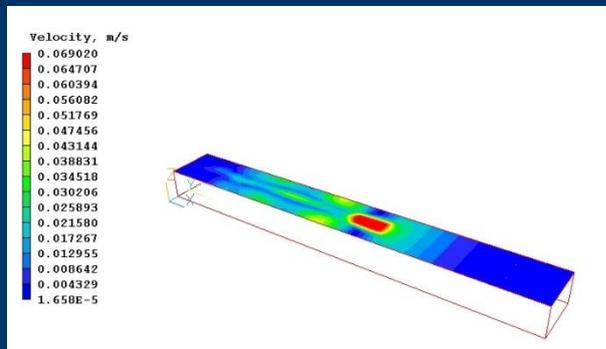

Figure 4. Surface velocity plot after 16s showing location of moving body. Bottom, density profile results (tank walls) after 16s from the moving body method incorporating the body equation of motion (compare with figure 1).

Figure 5 illustrates how the total force on the moving object (RPH method) is reduced in the stratified case due to the increased drag resulting from generation of internal waves. For further details on the implications of this effect, see ref 1
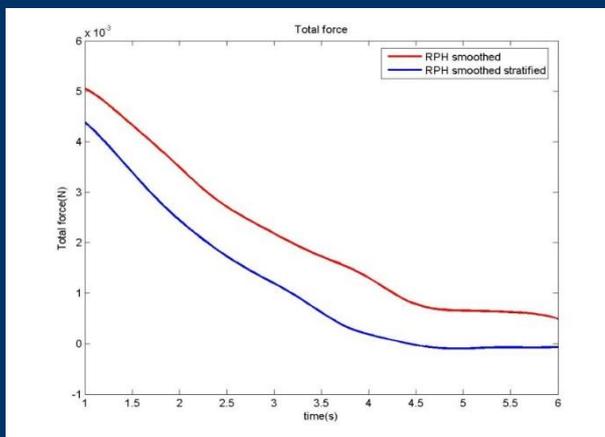
Figure 6. Comparison of total force on object moving in tank with uniform density of 1000kg/m-3 (red) and in the tank stratification illustrated in figure 1 (blue).

Conclusions

A moving-body method similar to MOFOR has been developed and shown to work well. The method allows either a specified body position with time to be set or a body movement under the action of specified forces. It allows a useful extension to MOFOR.

Dr R P Hornby email: bob.hornby007@gmail.com

References

1. Hornby R P. PHOENICS Modelling of the 'Dead Water' Effect. PHOENICS Newsletter Spring/Summer 2009.

CFD investigations for reducing personal exposure to particulates emitted from residential Chinese cooking. By Yuejing Zhao+, Bin Zhao and Michael Malin* +Department of Building Science, School of Architecture, Tsinghua University, Beijing 100084, China. *Concentration, Heat And Momentum Limited (CHAM), Wimbledon Village, SW19 5AU. Jan 2020 – PH-2018.

Cooking is known to be a major source of indoor particulate matter (PM), particularly in Chinese households (Abdullahi et al., 2013; Zhao and Zhao, 2018). When compared with Western residential cooking, the indoor air pollution generated by Chinese cooking is much more severe owing to the special cooking style; for this reason it has become an important influential factor on indoor air quality in Chinese residences. Chen et al (2018) found that the high temperatures of over (170°C) required for some traditional Chinese cooking methods, such as stir-frying, pan-frying, and deep-frying, generate high levels of fine particulate matter under 2.5 μm (PM2.5).

Studies have associated development of lung cancer among Chinese women, including non-smoking women, with their exposure to cooking oil fumes (COF) (Hung et al, 2007; Wang et al, 2014). Some measured data show that, even with the cooker range-hood operating, the PM2.5 concentration in the kitchen could still reach over 500 μg/m^3 with bad ventilation (Chen et al, 2018).

The overall objective of this research was to explore possible control measures of air pollution during cooking by using PHOENICS-FLAIR to simulate PM2.5 levels in a typical residential arrangement, as shown in the kitchen and adjacent living room depicted in Figure 1.

Model Description

The kitchen contains a cooker, cooking pan, range hood, open window, and open doorway to the living room. Other neighbouring rooms, including the bathroom, were not explicitly in the CFD model; but rather they were represented in terms of open doorways with constant low-level inflow and high-level outflow boundaries, whose volume flow rates and incoming time-varying PM2.5 concentrations in μg/m^3 were determined by the multi-zone computer program CONTAMW3 (Dols & Polidoro, 2015). The multi-zone model uses the well-mixed assumption for each room to calculate airflow, energy and species transport between the rooms of a building, and between the building and outdoors. Further information on its use in the present study has been given by Zhao and Zhao (2019).

The range hood was defined by a constant volume extraction rate of 530 m^3/hr, and the cooking pan was modelled as a heat source of 2.5kW with a PM2.5 emission rate of 5 mg/min. The external ambient temperature was taken as 25°C, and the open window of the kitchen was defined as a pressure boundary at atmospheric pressure.

The kitchen measures 1.6m by 3.5m by 2.8m, and the adjoining living room 3m by 4.5m by 2.8m. Zhao and Zhao (2019) used a breathing space with dimensions 0.25m x 0.5m x 0.5m, the centre of which was 1.5m and 1.2m above the floor in the kitchen and living room respectively, to determine the average PM2.5 concentration in each room between different cases.

Gravitational effects were represented by means of the reduced-pressure formulation, where buoyancy forces appear in the momentum equation in terms of a perturbation density from ambient. Turbulence was represented by means of the standard k-ε model with empirical wall functions.

The Ideal Gas law was used to obtain the variation of air density with temperature, and the drift-flux model was applied to represent particle transport and its slippage relative to the air due to gravitational effects (Zhao *et al.*, 2009; Zhou and Zhao, 2011).
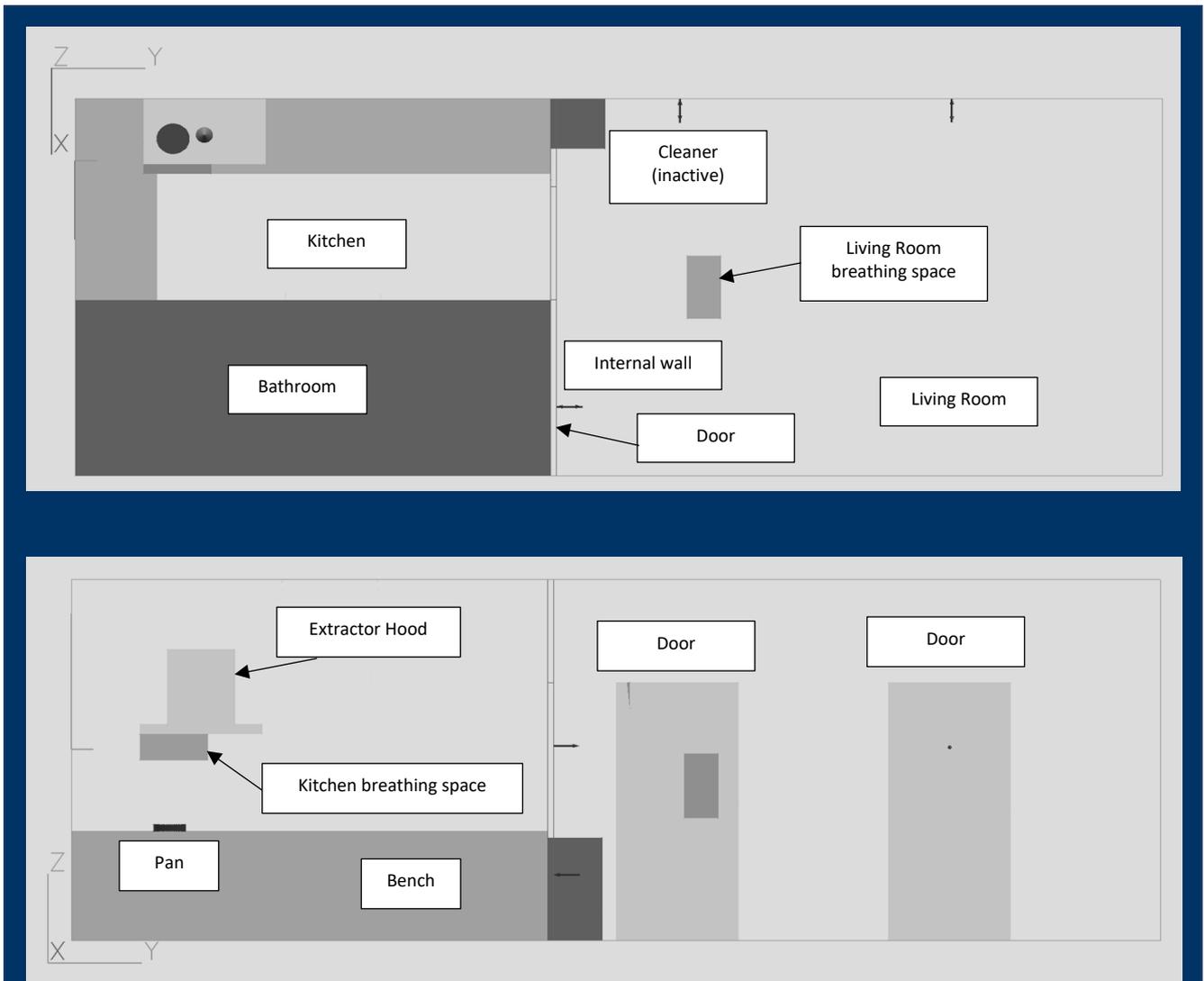
Figure 1: Plan (top) and front (bottom) elevation of the model layout showing position and size of all major structures.

Results and Discussion

Zhao and Zhao (2019) considered first a base case, and then a further eight cases to study the effect of two types of control measure for improving air quality, namely: (a) configuring a ceiling screen in the kitchen to obstruct COF pervasion; and (b) employing an air cleaner in the living room and/or kitchen to remove PM2.5. The different cases varied the positioning of the ceiling screen and air cleaners. Steady-state solutions were performed to produce the flow and thermal solution fields in the absence of particles. For each case a transient restart simulation was performed from the steady solution to predict the temporal evolution of the particle concentration field. The transient simulation covered 10 minutes duration using a time step of 1s. Figures 2 to 3 show some typical CFD results for the base case in terms of temperature contours and PM2.5 iso-surface contours, respectively. In Figure 2, temperatures beyond the contour limit of 30°C are displayed as the limit colour; and the figure also includes velocity vectors that are capped at 0.5 m/s for clarity, although this is exceeded only just below the extractor hood.
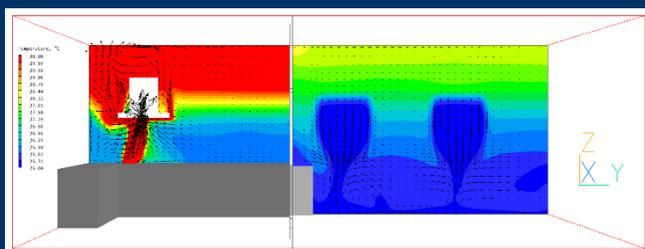

Figure 2: Temperature contours and velocity vectors across the kitchen and living room in the X-plane in line with the extraction hood.

The iso-surface in Figure 3 corresponds to a PM2.5 value of 60 µg/m^3. This figure serves to illustrate the progression of cooking-oil particulates from the kitchen and into the living-room space.

Figure 3: Iso-surface plot of PM2.5 concentration (60 µg/m3) coloured by temperature.
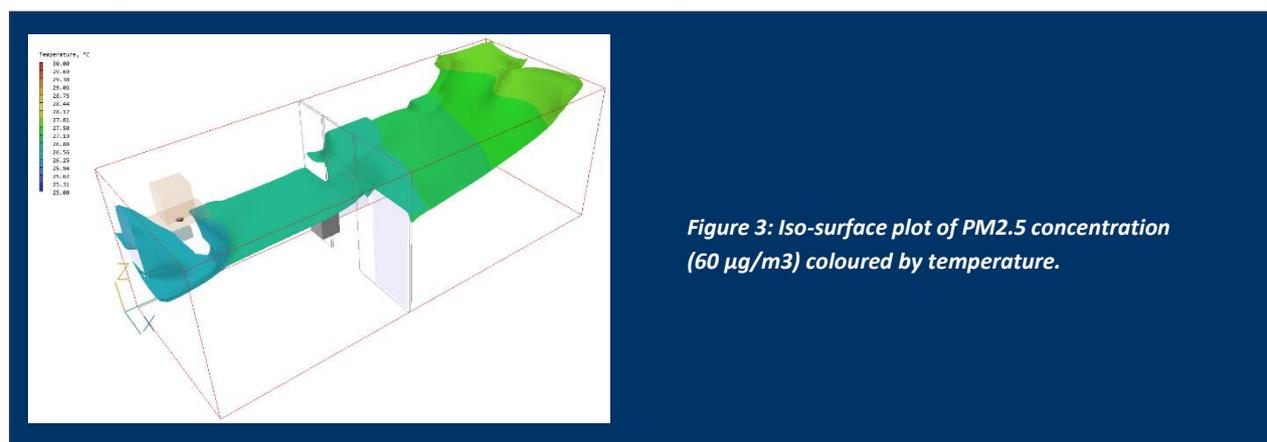
The results of this, and all other cases, were highlighted and discussed in detail in the paper of Zhao and Zhao (2019), including reports on the effects of different control measures. For example, the use of ceiling screens in the kitchen was found to reduce the PM2.5 concentration in the living room by up to 10%, depending on the number of screens and their location. Not surprisingly, the use of an air cleaner significantly improved the air quality in the living room; some further improvement was obtained when using both control measures.

Conclusions

This type of research has shown how PHOENICS-FLAIR can be used to provide insight into the flow, temperature and concentration fields generated by residential cooking. These results can then be used to provide some guidance in engineering-control strategies of air pollution. Further reading can be found in the experimental paper of Zhao and Zhao (2020); and in the references cited, including the original CFD study of Zhao and Zhao (2019).

References

Abdullahi K. L., et al, 2013. Emissions and indoor concentrations of particulate matter and its specific chemical components from cooking: A review. *Atmospheric Environment*, 71: 260-294.

Chen C., et al., 2018. Emission Rates of Multiple Air Pollutants Generated from Chinese Residential Cooking. *Environmental Science & Technology*, 52(3): 1081-1087.

Dols W.S. and Polidoro B.J. 2015. CONTAM user guide and program documentation. Version 3.2, NIST Technical Note 1887, National Institute of Standards and Technology, Gaithersburg, MD, USA.

Hung H. S., et al., 2007. Association of cooking oil fumes exposure with lung cancer: Involvement of inhibitor of apoptosis proteins in cell survival and proliferation in vitro. *Mutation Research-Genetic Toxicology and Environmental Mutagenesis*, 628(2): 107-116.

Wang X., et al., 2014. Lung cancer risk assessment of cooking oil fume for Chinese non-smoking women. *WIT Transactions on the Built Environment*, 145: 243-250.

Zhao B., et al., 2009a. Modelling of ultrafine particle dispersion in indoor environments with an improved drift flux model. *Journal of Aerosol Science*, 40(1): 29-43.

Zhao B., et al., 2009b. How Many Airborne Particles Emitted from a Nurse will reach the Breathing Zone/Body Surface of the Patient in ISO Class-5 Single-Bed Hospital Protective Environments - A Numerical Analysis. *Aerosol Science and Technology*, 43(10): 990-1005.

Zhao Y. J., Zhao B., 2018. Emissions of air pollutants from Chinese cooking: A literature review. *Building Simulation*, 11(5): 977-995.

Zhou B., Zhao B., 2011. Test of a generalized drift flux model for simulating indoor particle dispersion. *Proceedings of ISHVAC 2011, Vols I-IV*, pp. 382-387, Shanghai, China.

Zhou B., et al., 2016. Study on pollution control in residential kitchen based on the push-pull ventilation system. *Building and Environment*, 107: 99-112.

Zhao Y., Zhao B., 2019. Investigations for Reducing Personal Exposure to PM2.5 from Residential Chinese Cooking Based on CFD Simulation, 11th *Proceedings of ISHVAC 2019,* Harbin, China.

Zhao Y., Zhao B., 2020. Reducing human exposure to PM2.5 generated while cooking typical Chinese cuisine, *Building and Environment*, Volume 168, 106522

The University of Ljubljana recently published two papers [1,2] documenting the results of their research into the thermal response and energy-saving capabilities of multi-layer glass and building-integrated-photovoltaic (BIPV) façade structures in different climate conditions. This work has been performed in the context of the European Union's Energy Performance Building Directive (EPBD) [3] that requires all new buildings to be nearly Zero-Energy Buildings (nZEB) from 2021 onwards.

Despite progress in energy performance in recent decades buildings remain significant energy consumers. Advanced technologies to increase energy efficiency have been developed, and strong commitments to increasing energy performance adopted. Medved et al [1] present evaluation methods and energy performance of advanced facade building structures comprising six-pane multi-layer glass with optional photovoltaic cells integrated in the outer glass layer (BIPV). Four sealed cavities contain argon and one air (Figure 1). All glass panes have a one-side low emissivity layer meaning the glazed façade structure will have thermal transmittance comparable to well thermally insulated, in-built, opaque walls.

Figure 1: 6 pane glass façade structure designed for all-glass buildings (left) [4], multi-layer glass and BIPV façade structure studied in the article on the test stand (right) [1].

The dynamic thermal response model of multi-layer glass/BIPV façade structures was simulated by:

1. Determination of steady state optical and thermal properties of a multi-layer glass façade structure using WINDOW 7.6.
2. Definition of virtual time-dependant boundary conditions including solar irradiation, indoor and outdoor air temperature in the form of six virtual days that corresponds to various climate conditions and orientations of the façade structure.
3. Determination of pressure, velocity, temperature fields and turbulent energy in 300-second time steps over the length of 24 hours using the PHOENICS 2018 CFD code.
4. Determination of specific heat flux at the inner surface of multi-layer glass and BIPV façade structures as a linear time series using a black-box method and machine-learning. Regression models like this can enable fast modelling of the thermal response and energy needs of all-glass buildings.

The models in Medved et al [1] were developed solely to evaluate energy performance of facade structures. Domjan et al [2] took this further to determine energy demand decreases and study the effect of natural and hybrid (mechanical) ventilation. A BIPV$_{100}$ façade structure is one where the photovoltaic (PV) cell area corresponds to 60% of the multi-layer glass structure area. Figure 2 shows temperature distribution during dynamic model for multi-layer glass and BIPV$_{100}$ structures, alongside some wider context of the simulations.

Medved et al [1] validated their model against experimental results and showed that the proposed approach is significantly more accurate than massless dynamic models. The study provides a solid basis for further research of advanced technologies for nearly nZEBs and beyond. Although the models in the article were developed solely to evaluate energy performance of facade structures, models can be integrated into computer tools to determine the dynamic thermal responses of buildings to provide more accurate analysis of an all-glass building with advanced multi-layer glass and BIPV facade structures.

Domjan et al [2] show that final energy demand decreases by 17–37% compared with the reference all-glass building by using these structures. In all-BIPV buildings, final energy demand is decreased by 36–48%. Such buildings can

contribute significantly to the mitigation of global climate change, as BIPV electricity production exceeds building energy demand.
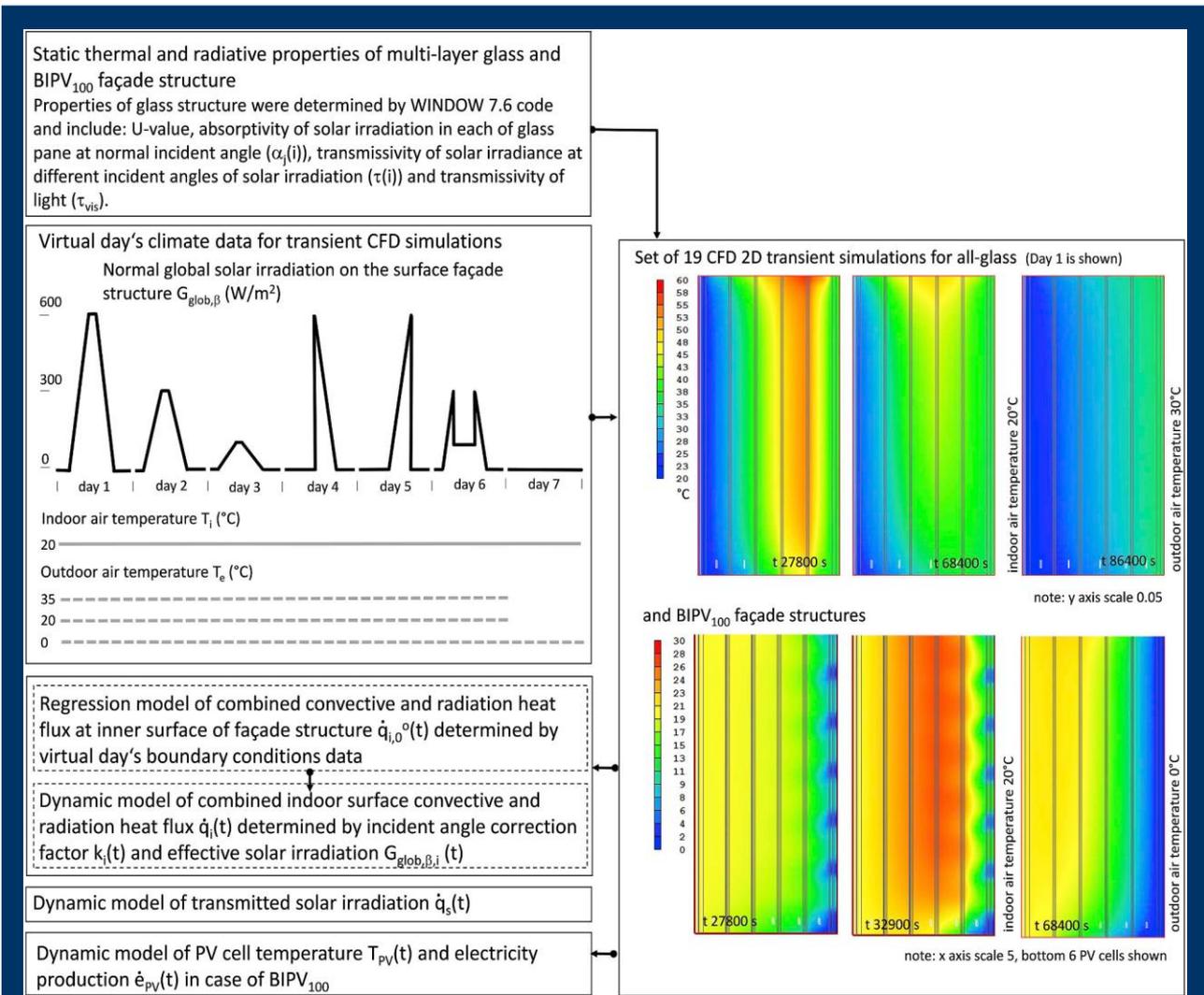
Static thermal and radiative properties of multi-layer glass and BIPV$_{100}$ façade structure
Properties of glass structure were determined by WINDOW 7.6 code and include: U-value, absorptivity of solar irradiation in each of glass pane at normal incident angle ($\alpha_j(i)$), transmissivity of solar irradiance at different incident angles of solar irradiation ($\tau(i)$) and transmissivity of light (τ_{vis}).

Virtual day's climate data for transient CFD simulations

Normal global solar irradiation on the surface façade structure $G_{glob,\beta}$ (W/m^2)

Indoor air temperature T_i (°C)

Outdoor air temperature T_e (°C)

Set of 19 CFD 2D transient simulations for all-glass (Day 1 is shown)

and BIPV$_{100}$ façade structures

note: y axis scale 0.05

note: x axis scale 5, bottom 6 PV cells shown

Regression model of combined convective and radiation heat flux at inner surface of façade structure $\dot{q}_{i,0}{}^o(t)$ determined by virtual day's boundary conditions data

Dynamic model of combined indoor surface convective and radiation heat flux $\dot{q}_i(t)$ determined by incident angle correction factor $k_i(t)$ and effective solar irradiation $G_{glob,\beta,i}(t)$

Dynamic model of transmitted solar irradiation $\dot{q}_s(t)$

Dynamic model of PV cell temperature $T_{PV}(t)$ and electricity production $\dot{e}_{PV}(t)$ in case of BIPV$_{100}$

Figure 2: hematic description of the procedure developed for the determination of dynamic response models of all-glass and BIPV100 façade structures. [2]

Figure 3 shows the results of the dynamic thermal response simulation and experimental data for both the multi-layer glass and BIPV$_{100}$ structure. This shows good agreement and successfully validates the simulation.
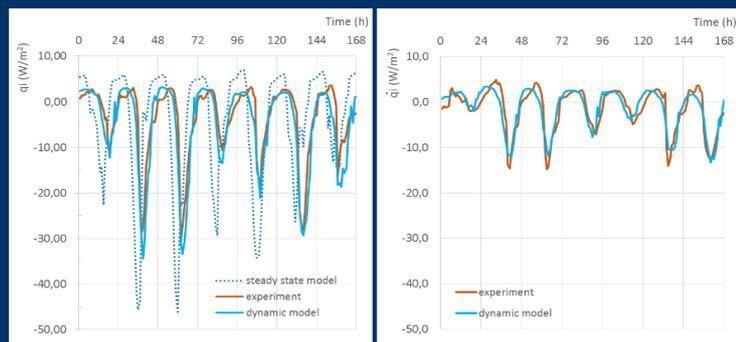
References

1) Medved,S. et al, "The dynamic thermal response model and energy performance of multi-layer glass and BIPV façade structures", Energy & Buildings 188–189 pp.239–251 (2019)
2) Domjan,S., et al, "Evolution of all-glass nearly Zero Energy Buildings with respect to the local climate and free-cooling techniques", Building and Environment 160, 106183, (2019).
3) Energy Performance of Building Directive (Directive 2010/31/EU), 2018/844, EC, (2018)
4) Drev,M. Černe,B. Žnidaršič,M. Geving,A., "Nearly independent, near-zero energy building" (2018) https://www.researchgate.net/publication/320876196

1. Comfort in a meeting room

A new ventilation system needed to be developed for a meeting room in a town hall where fresh air was supplied through diffusors in the ceiling and exhaust air flowed through shadow gaps at the ceiling along the room. The room had a cooled ceiling (summer) and floor heating (winter).

PHOENICS/FLAIR was used to evaluate various diffusor types and positions, air flows and air temperatures to ensure a good comfort in winter and summer. The advantage of being able to visualise PMV and PPD according to the ISO 7730 standard was very useful.

Temperature distribution just above the floor and streamlines in the bedroom during the summer
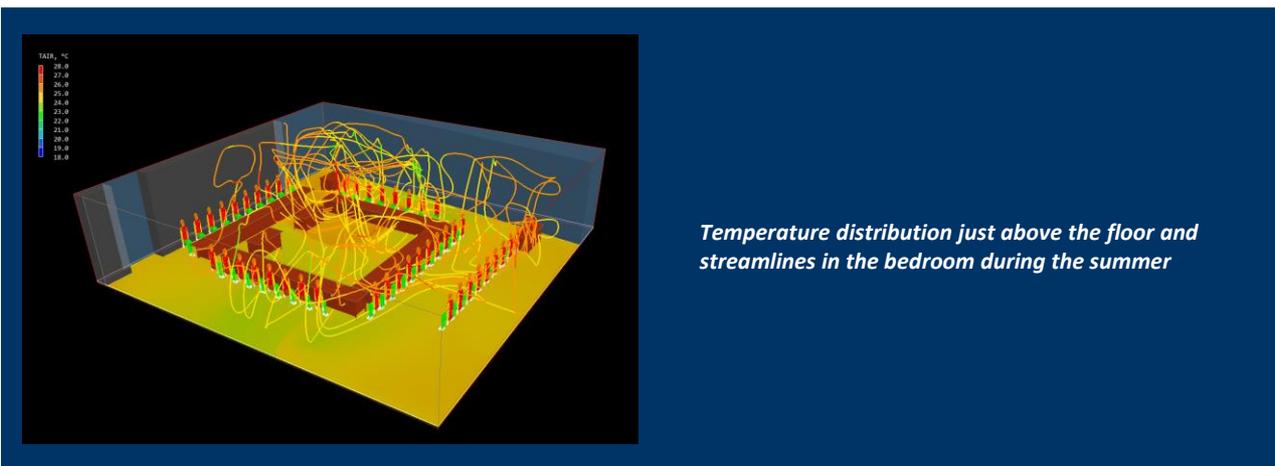
2. High-performance data centre

Cooling high-performance data centres is power-hungry; it is therefore crucial that it is done efficiently.

In this particular data centre the underfloor conditioned air entered the cold aisle through perforated floor tiles; the cold air was pulled into the front of the rack mount equipment using fans. At the same time, exhaust left the rear of the rack mount equipment and exited the enclosure into the hot aisle. Servers were set up in the racks back to back and the warm isles were isolated from the rest of the room. By that energy-critical "air short circuit" gets prevented.

PHOENICS/FLAIR was used to calculate temperature and velocity distribution for normal operation and during an "accident" where only half of the air flow is available.

Based on these simulations a number of design changes could be suggested to improve cooling effectiveness and robustness in case of a failure.


Data Centre temperature distribution
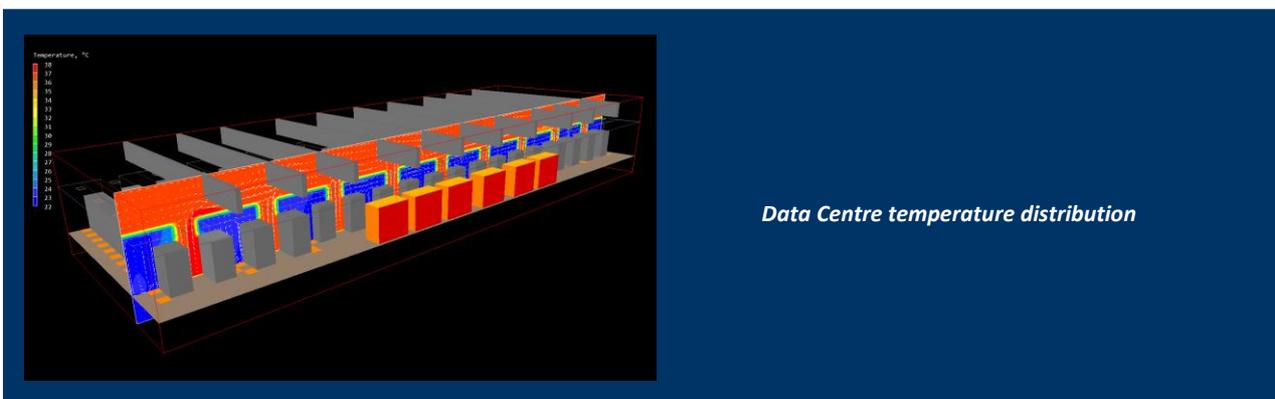
3. Old track hall

As part of renovation planning for an old track hall, existing wind loads needed to be determined. PHOENICS wind - load simulations were carried out for 3 flow directions: transverse, longitudinal and under 45°.

Wind loads were expressed as net pressure coefficients defined as the difference at the out- and inside of local pressure on the construction divided by the dynamic head at the wind reference velocity. The pressure coefficients were used by a design engineer to construct a renovated track hall capable of withstanding all future storms.
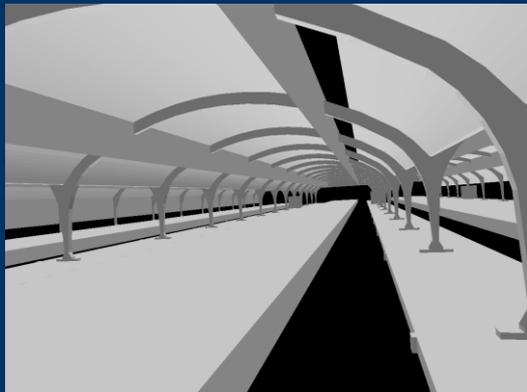
Old Track Hall
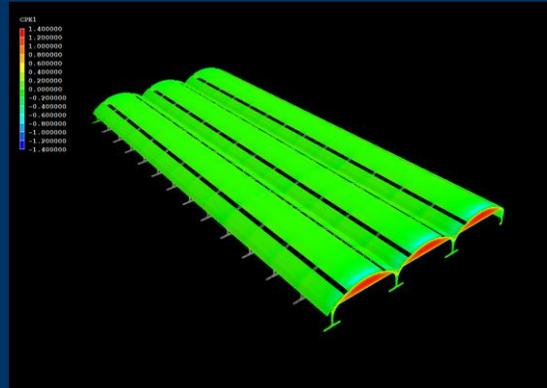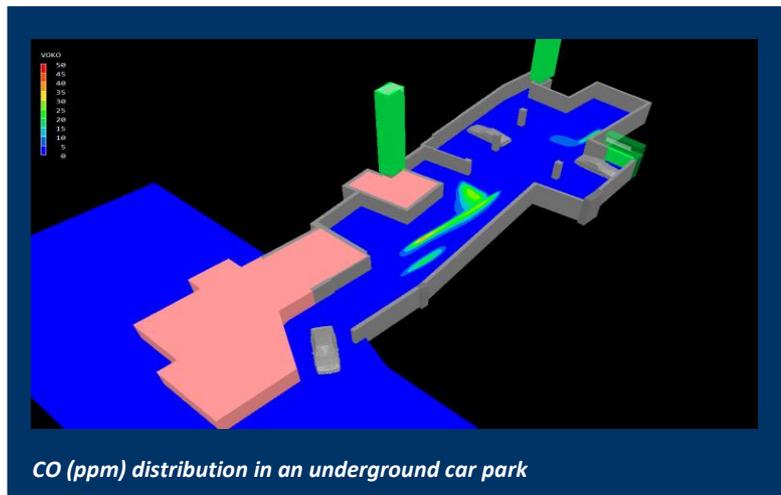

Pressure coefficients on the track hall

4. CO concentrations in an underground park

A small private underground car park needed checks to determine if it needed an expensive ventilation system installed.

Local authorities would approve the non-installation of said system only if the owner could prove that natural ventilation of the underground car park ensured a 0.5-fold air change and that the half-hour average CO concentration of 50 ppm was not exceeded for a scenario with three car trips within 30 minutes.

It was agreed to perform PHOENICS transient calculations for two atmospheric

CO (ppm) distribution in an underground car park

conditions: one with a wind speed of 3.6 m/s from west-northwest and one when there was no wind. Outside temperature was set to 20ºC.

It was proved that, for both cases, the requirements of the local authorities were met.

5. Keeping snow fresh in a ski hall

Snow was melting too quickly in a ski hall because of overly high air temperatures just above the snow deck. It was decided to remove the old ventilation system and use PHOENICS to design a new system.

Several designs were evaluated using PHOENICS. The high outside temperatures (over 35ºC) and the high number of people inside the hall made it extremely difficult to fulfil the inside air temperature demands and still keep the climate comfortable (no draughts) for visitors.

With the use of PHOENICS it has been possible to find the optimal system.
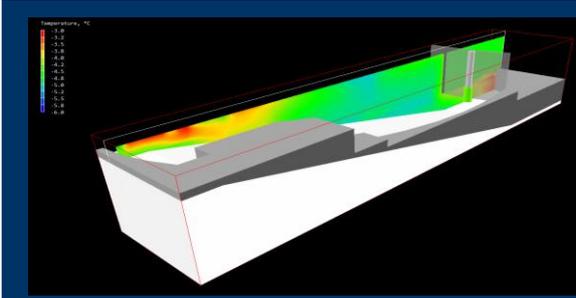
Temperature distribution in a ski hall

News from CHAM: Sponsoring a Local School

Last year CHAM part-sponsored Ricards Lodge High School, a single sex comprehensive secondary school for girls from 11 – 16 located in Wimbledon. This year CHAM is fully sponsoring the School.

Sponsorship relates to a programme run through Dendrite Connect by The Learning Partnership (https://www.thelearningpartnership.com/). Schools are linked worldwide and students have the opportunity to participate in a variety of challenges one of which is *Race to the Line* relating to Model Rocket Cars. School Teams build, and race, cars locally, nationally and internationally. Last year some 200 students from Ricards Lodge were involved and made the national finals. They hope to repeat their success this year. Students will construct their cars this term and race day will take place in March.

CHAM will attend the in-School race day and, perhaps, regional and national events as the students progress. #CHAM #RFTLUK #RTTLUK @dendrite_me @The Learning Partnership @Dendrite Learning Platform.

Contact CHAM

Should you require further information on any of our offered products or services, please give us a call on +44 (20) 8947 7651. Alternatively, you can email us on: sales@CHAM.co.uk

Our website can be viewed at www.CHAM.co.uk and we can be found on the following social media platforms:

Concentration Heat and Momentum Limited (CHAM)
Bakery House
40 High Street
Wimbledon Village
London SW19 5AU, England.